

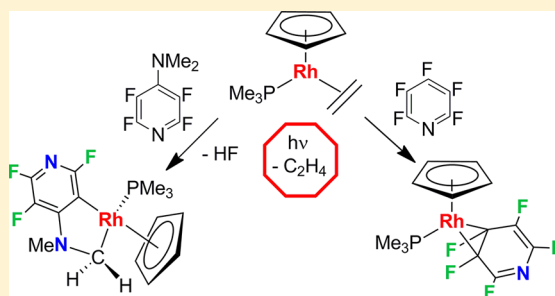
Photochemical Reactions of Fluorinated Pyridines at Half-Sandwich Rhodium Complexes: Competing Pathways of Reaction

Barbara Procacci, Robin J. Blagg,[†] Robin N. Perutz,* Nuria Rendón,[‡] and Adrian C. Whitwood

Department of Chemistry, University of York, York, U.K. YO10 SDD

Supporting Information

ABSTRACT: Irradiation of CpRh(PMe₃)(C₂H₄) (1; Cp = η⁵-C₅H₅) in the presence of pentafluoropyridine in hexane solution at low temperature yields an isolable η²-C,C-coordinated pentafluoropyridine complex, CpRh(PMe₃)(η²-C,C-C₅NF₄) (2). The molecular structure of 2 was determined by single-crystal X-ray diffraction, showing coordination by C3–C4, unlike previous structures of pentafluoropyridine complexes that show N-coordination. Corresponding experiments with 2,3,5,6-tetrafluoropyridine yield the C–H oxidative addition product CpRh(PMe₃)(C₅NF₄)H (3). In contrast, UV irradiation of 1 in hexane, in the presence of 4-substituted tetrafluoropyridines C₅NF₄X, where X = NMe₂, OMe, results in elimination of C₂H₄ and HF to form the metallacycles CpRh(PMe₃)(κ²-C,C-CH₂N(CH₃)C₅NF₃) (4) and CpRh(PMe₃)(κ²-C,C-CH₂OC₅NF₃) (5), respectively. The X-ray structure of 4 shows a planar RhCCNC-five-membered ring. Complexes 2–5 may also be formed by thermal reaction of CpRh(PMe₃)(Ph)H with the respective pyridines at 50 °C.



INTRODUCTION

There has been substantial recent progress in C–F bond activation of aromatic and alkene C–F bonds in both stoichiometric and catalytic reactions.¹ Transition-metal-mediated C–F bond activation holds out the prospect of new ways of making fluorocarbons. It has also been found to be an excellent method of generating metal fluoride complexes.^{1c} The analogy to C–H bond activation is tempting, but the contrasts can also be revealing. While cyclometalation via C–H bond activation is common, few examples of cyclometalation via C–F activation have been reported.

Albrecht reviewed cyclometalation reactions using d-block transition metals, showing many examples of metallacycles successfully applied in organic transformations, in catalysis and in various other domains of materials science.² Since then, many other papers have been published presenting characterizations of new metallacycles,³ applications in hydrodefluorination catalysis,⁴ oxygen sensing,⁵ and transfer hydrogenation.⁶

C–F activation reactions to form a metallacycle have been achieved thermally using a Co(I) center with an aldazine N atom as an anchoring group to afford an ortho-chelated cobalt(III) complex containing a [C–Co–F] fragment;⁷ Li and co-workers also reported a reaction where a cobaltacycle is formed after C–F activation and new fluoro-organics are formed by subsequent carbonylation reactions.⁸ OsO₄ reacts in the presence of HSR (R = C₆F₅, C₆F₄H-4) to afford different metallacycles through a process involving the rupture of one or two C–F bonds.⁹ Love et al. have also demonstrated the activation of a C–F bond in the position ortho to an imine substituent of polyfluorinated arenes at platinum. Formation of a cyclometalated Pt complex leads to the methylation of

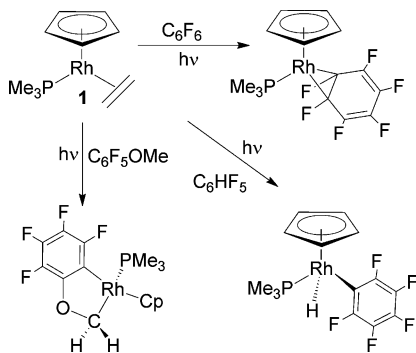
polyfluorinated aryl imines by subsequent transmetalation and reductive elimination steps.¹⁰ In all of these reactions, the ligands coordinate to the metal center first through the heteroatom (N or S) and the C–F bond is cleaved subsequently. A metal fluoride is detected in all the preceding examples except the osmium complex, either as the final product or as an intermediate in the catalytic cycle. No formation of HF has been detected or mentioned as a side product in any of these publications.

The use of rhodium for C–F activation reactions has been recently reviewed by Braun et al.;^{1d} phosphine–rhodium complexes show particular effectiveness in C–F activation. Yamaguchi and co-workers reported C–F activation of fluorinated arenes and pyridines at rhodium centers;¹¹ Braun et al. found that RhH(PET₃)₃ is capable of stoichiometric C–F activation in the 4-position of pentafluoropyridine.¹² More recently, they also prepared a 16-electron Rh(I) boryl complex, capable of ortho C–F activation of pentafluoropyridine. Calculations suggested a boryl-assisted mechanism and showed that the regioselectivity derives from nitrogen participation in the transition state.¹³ Attack on a η⁵-pentamethylcyclopentadienyl rhodium(III) complex occurred at the less activated position, meta to the ring nitrogen atom, of a tetrafluoropyridyl substituent of a coordinated N-heterocyclic carbene.¹⁴

The photochemistry of CpRh(PMe₃)(C₂H₄) (1, Cp = η⁵-C₅H₅; Scheme 1) has already been explored extensively at room temperature. Upon photolysis, loss of ethene leads to the formation of an unsaturated 16-electron complex capable of

Received: June 14, 2013

Published: December 31, 2013

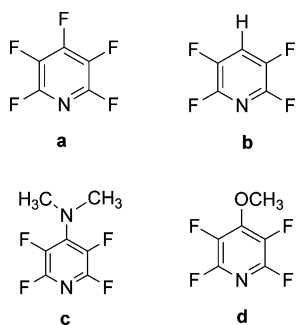
Scheme 1. Photoreactions of **1** with Fluorinated Arenes

activating a wide range of bonds.¹⁵ It reacts with benzene to yield $\text{CpRh}(\text{PMe}_3)(\text{C}_6\text{H}_5)\text{H}$ via a short-lived η^2 -arene complex. Photolysis with C_6F_6 results in the isolation of the stable η^2 -hexafluorobenzene complex $\text{CpRh}(\text{PMe}_3)(\text{C}_6\text{F}_6)$,¹⁶ and reaction in pentafluoroanisole generates the metallacycle $\text{CpRh}(\text{PMe}_3)(\kappa^2\text{-C,C-CH}_2\text{OC}_6\text{F}_4)$, characterized by multinuclear NMR spectroscopy; reaction of this complex with 1 equiv of $[\text{Ph}_3\text{C}]^+[\text{PF}_6]^-$ at 220 K generates $[\text{Cp}(\text{PMe}_3)\text{Rh}=\text{C}(\text{H})\text{-OC}_6\text{F}_4]\text{PF}_6$.

C–F bond cleavage of hexafluorobenzene has been achieved in the reaction with $\text{Cp}^*\text{Rh}(\text{PMe}_3)(\text{C}_2\text{H}_4)$ ($\text{Cp}^* = \eta^5\text{-C}_5\text{Me}_5$). C–F activation took place upon further photolysis following initial η^2 coordination of hexafluorobenzene.¹⁸ Studies in Ar matrices at 12 K confirmed that while $\text{CpRh}(\text{PMe}_3)(\eta^2\text{-C}_6\text{F}_6)$ prefers to eliminate C_6F_6 to form the 16-electron fragment, the more crowded $\text{Cp}^*\text{Rh}(\text{PMe}_3)(\text{C}_2\text{H}_4)$ produces the C–F activated product preferentially.¹⁹ Both the thermally generated fragment $\text{Cp}^*\text{Rh}(\text{PMe}_3)$ and the photochemically generated fragment $\text{CpRh}(\text{PMe}_3)$ react with fluorinated aromatic hydrocarbons to yield the C–H activated products $\text{Cp}^*\text{Rh}(\text{PMe}_3)\text{-}(\text{aryl}_\text{F})\text{H}$ when an aromatic C–H bond is present.²⁰

In this paper, we explore the behavior of complex **1** in the presence of pentafluoropyridine, 2,3,5,6-tetrafluoropyridine, and substituted analogues (Scheme 2, compounds a–d) to

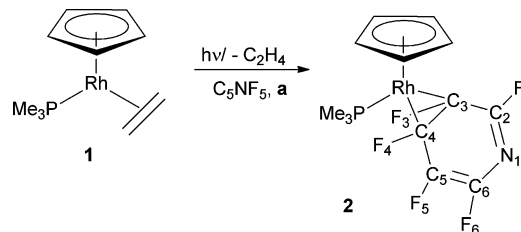
Scheme 2. Fluorinated Heteroaromatics Investigated



obtain information about coordination modes, substituent effects, and reaction mechanisms. Reaction with pentafluoropyridine (**a**) allowed us to isolate and characterize $\text{CpRh}(\text{PMe}_3)(\eta^2\text{-C}_5\text{NF}_5)$ (**2**), whereas reaction with 2,3,5,6-tetrafluoropyridine (**b**) formed the C–H activated product $\text{CpRh}(\text{PMe}_3)(\text{C}_5\text{NF}_4)\text{H}$ (**3**) selectively. We report the formation of the two metallacycles **4** and **5** by intramolecular C–F activation of 4-substituted tetrafluoropyridines (**c** and **d**) at the Rh center.

RESULTS

Irradiation of 1 with Pentafluoropyridine (a). The irradiation of **1** in hexane with excess pentafluoropyridine ($\lambda > 290$ nm, 8 h, room temperature) generates a large number of products. When the reaction is performed at low temperature (-20 °C), the formation of one complex is preferred, leading to an NMR yield for complex **2** of >60%. At early times, **2** is the only product detected by NMR spectroscopy. This product was purified by removal of **1** by sublimation followed by crystallization, giving an orange product characterized by multinuclear NMR spectroscopy, high-resolution EI mass spectrometry, and X-ray crystallography. The $^{31}\text{P}\{^1\text{H}\}$ NMR spectrum shows a resonance at δ 3.09, as a doublet of doublets of doublets ($J_{\text{RhP}} = 192$, $J_{\text{PF}} = 56$, 52 Hz). The value of J_{RhP} indicates a Rh(I) oxidation state,¹⁶ and the large values of J_{PF} are similar to those for $\text{Rh}(\eta^2\text{-C}_6\text{F}_6)$ complexes.¹⁶ We therefore assign complex **2** as $\text{CpRh}(\text{PMe}_3)(\eta^2\text{-C}_4\text{F}_5\text{N})$ with the pentafluoropyridine bonded in an $\eta^2\text{-C,C}$ mode. The distinction between coordination at C3–C4 and C2–C3 may be made through the ^{19}F NMR spectrum. The $^{19}\text{F}\{^{31}\text{P}\}$ NMR spectrum allowed the exact assignments for the five inequivalent fluorines on the pyridine ring. The two fluorines close to N (F_2 , F_6) resonate at lower field at δ -55.5 and δ -119.8 , F_5 , which is not involved in the η^2 coordination, resonates at δ -155.7 , and the two remaining fluorines appear at δ -157.3 (F_4) and δ -169.0 (F_3) (Scheme 3).

Scheme 3. Photochemical Formation of **2**

from ^{31}P were observed just for F_3 and F_4 , confirming that these two fluorines are bound to the coordinated carbons involved in η^2 coordination. The evidence from NMR spectroscopy indicates that the pentafluoropyridine is coordinated in a $\eta^2\text{-C}_3\text{C}_4$ fashion. Selected NMR data for complex **2** are given in Table 1.

The crystal structure of **2** shows the coordination of pentafluoropyridine but is complicated by disorder between the C6 (and F6) and the N1 of the pyridine ring (Figure 1a). The occupancies of the two conformers refined to 0.690:0.310(12). The structure of **2** shows a planar C_5NF_3 unit with the two C–F bonds involved in the η^2 coordination bent out of the plane by $42.09(2)^\circ$ (Figure 1b) in comparison to 43.8° for the $\text{Rh}(\eta^2\text{-C}_6\text{F}_6)$ analogue reported previously.¹⁶ Similarly, the angle between the planes $\text{RhC}(3)\text{C}(4)$ and $\text{C}(2)\text{C}(3)\text{C}(4)\text{C}(5)\text{C}(6)\text{N}(1)$ is $106.70(16)^\circ$ in comparison to 108.6° for the $\text{Rh}(\eta^2\text{-C}_6\text{F}_6)$ analogue. These interplane angles have been demonstrated to be very characteristic of $\text{M}(\eta^2\text{-C}_6\text{F}_6)$ complexes.²¹ All the earlier crystal structures of coordinated pentafluoropyridine show the ligand bound through N, rather than $\eta^2\text{-C,C}$ as here.²² Johnson et al. have recently reported extensive NMR characterization of η^2 -coordinated pentafluoropyridine and tetrafluoropyridine at a nickel center.²³ Such complexes have often been proposed as

Table 1. NMR Data (δ (J/Hz)) in C_6D_6 for the Precursor and Photoproducts

	$^{31}P\{^1H\}$	1H	$^{19}F^a$
1	4.4 (d, $J_{Rh-P} = 200$)	0.77 (d, $J_{P-H} = 9.2$, PMe_3), 2.74 (m, C_2H_4), 1.46 (m, C_2H_4), 5.09 (s, Cp)	
2	3.0 (ddd, $J_{Rh-P} = 192$, $J_{P-F} = 56$, 52)	0.79 (d, $J_{P-H} = 10.5$, PMe_3), 4.37 (s, Cp)	-55.5 (m, F_2), -119.8 (t, $J_{F-F} = 11.4$, F_6), -155.7 (tdd, $J_{F-F} = 11.4$, 15.3, 34.3, F_3), -157.3 (m, F_4), -169.0 (m, F_3)
3	12.6 (d, $J_{Rh-P} = 142$)	-12.9 (dd, $J_{P-H} = 22.8$, $J_{Rh-H} = 40$, Rh-H), 1.35 (d, $J_{P-H} = 10.9$, PMe_3), 5.25 (s, Cp)	-100.7 (m, F_3 and F_4), -113.6 (m, F_2 and F_5)
4	13.8 (d, $J_{Rh-P} = 158$)	0.65 (d, $J_{P-H} = 10.6$, PMe_3), 2.96 (d, $J_{H-H} = 2.9$, CH_3), 3.04 (ddd, $J_{P-H} = 1.9$, $J_{Rh-H} = 6.7$, $J_{H-H} = 16.1$, H_A , CH_2), 4.87 (d, $J_{Rh-H} = 1.3$, Cp), 4.98 (dd, $J_{H-H} = 4.9$, 6.7, H_B , CH_2)	-66.5 (dd, $J_{F-F} = 12.7$, 23.7, F_2), -100.1 (dd, $J_{F-F} = 12.7$, 23.7, F_3), -180.2 (t, $J_{F-F} = 23.7$, F_4)
5	14.0 (d, $J_{Rh-P} = 159$)	0.54 (d, $J_{P-H} = 10.5$, PMe_3), 4.73 (d, $J_{Rh-H} = 1.3$, Cp), 5.12 (ddd, $J_{P-H} = 1.42$, $J_{Rh-H} = 5.40$, $J_{H-H} = 17.4$, H_A , CH_2), 6.77 (m, H_B)	-64.6 (dd, $J_{F-F} = 13.8$, 21.4, F_2), -99.1 (dd, $J_{F-F} = 13.8$, 21.4, F_3), -172.0 (t, $J_{F-F} = 21.4$, F_4)

^aThe fluorine atoms are numbered as for the corresponding X-ray structures. For 5, we follow the numbering of 4.

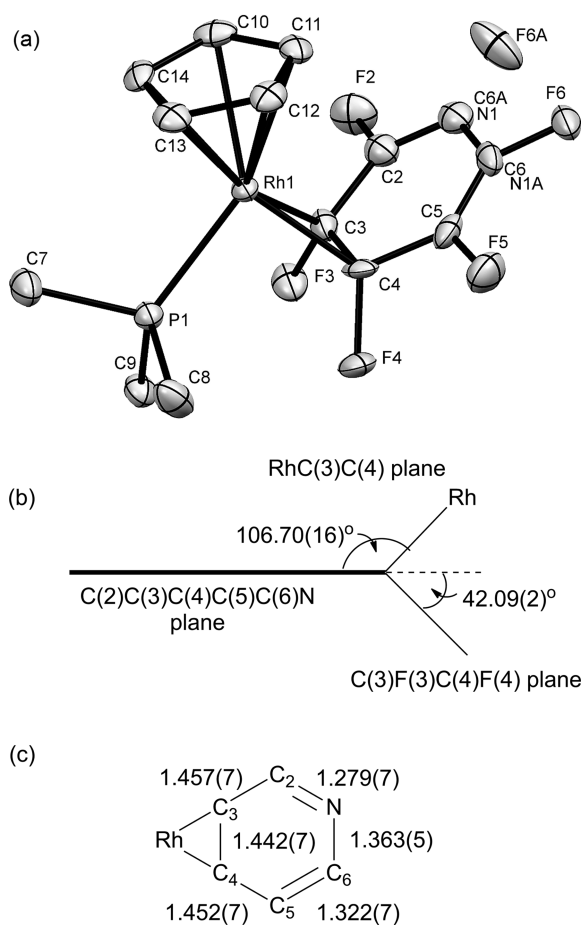


Figure 1. (a) Molecular structure of **2**. Hydrogen atoms are omitted for clarity. Ellipsoids for the anisotropic displacement parameters are shown at the 50% level. (b) Diagram showing interplane angles of the $Rh(\eta^2-C_5NF_5)$ unit. (c) Diagram of bond lengths (Å) for the η^2 -coordinated pyridine moiety (major conformer). Other bond lengths (Å): C(3)–Rh(1) 2.042(5), C(4)–Rh(1) 2.049(5), P(1)–Rh(1) 2.2732(10), C(2)–F(2) 1.332(6), C(3)–F(3) 1.382(6), C(4)–F(4) 1.381(5), C(5)–F(5) 1.339(6), C(6)–F(6) 1.310(6).

intermediates in C–F activation reactions (see the Discussion).^{16,17}

The coordinated C–C bond is extended to 1.442(7) Å. This may be compared to 1.379(4) Å for free C_5NF_5 determined in a solvate for the $Tp^*Rh(C_5NF_4)(PMe_3)FHF$ complex.²⁴ A diene pattern is observed for the uncoordinated C–C bonds of **2** (Figure 1c). The C–F bonds in the coordination positions (3 and 4) average 1.382(7) Å, an extension of about 0.05 Å in

comparison to the C–F bond length of free pentafluoropyridine (average 1.332(3) Å).²⁴

Irradiation of 1 with 2,3,5,6-Tetrafluoropyridine (b). The irradiation of **1** in C_6D_{12} with excess 2,3,5,6-tetrafluoropyridine (**b**) ($\lambda > 290$ nm, 8 h, room temperature) leads to the clean formation of product with a hydride resonance at $\delta -12.9$ (dd, $J_{P-H} = 22.8$, $J_{Rh-H} = 40.0$ Hz, Rh–H) and a doublet at $\delta 12.6$ (d, $J_{P-Rh} = 141.9$ Hz) in the $^{31}P\{^1H\}$ NMR spectrum, which was identified as $CpRh(PMe_3)(C_5NF_4)H$ (**3**). The ^{19}F NMR spectrum is consistent with two sets of equivalent fluorines in a 1:1 ratio, indicating unrestricted rotation about the Rh–C(pyridyl) bond. The NMR data are consistent with those found for the reaction of $CpRh(PMe_3)(C_2H_4)$ with partially fluorinated arenes.²⁰ Colorless crystals were grown by slow evaporation from hexane, and the crystal structure was determined (Figure 2). The hydride was located by a difference

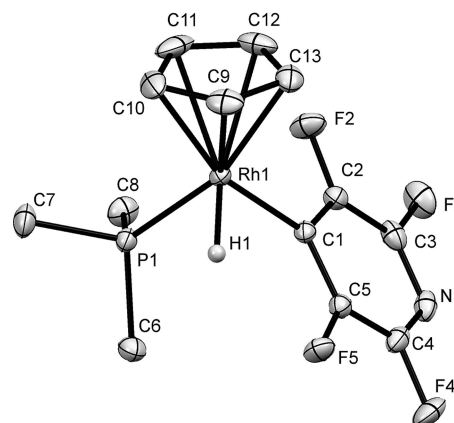


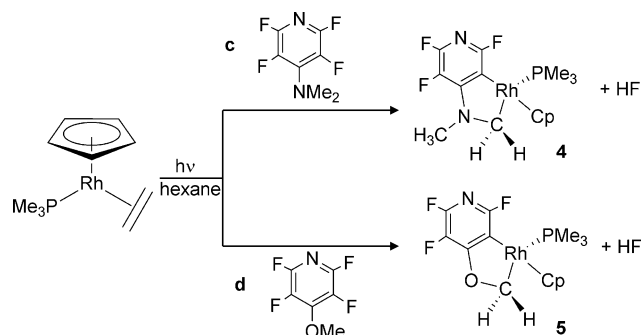
Figure 2. Molecular structure of **3**. Principal bond distances (Å): Rh(1)–C(1) 2.0363(18), Rh(1)–H(1) 1.53(3), Rh(1)–P(1) 2.2237(5). Principal angles (deg): C(1)Rh(1)P(1) 88.45(5), C(1)–Rh(1)H(1) 87.3(12). Hydrogen atoms other than hydride are omitted for clarity. Ellipsoids for the anisotropic displacement parameters are shown at the 50% level.

map. Treatment of **3** with CCl_4 resulted in the disappearance of the hydride resonance and formation of $CpRh(PMe_3)(C_5NF_4)Cl$ (**3-Cl**), which was also characterized by NMR spectroscopy and EI mass spectrometry. The $^{31}P\{^1H\}$ NMR spectrum of complex **3-Cl** shows a doublet of triplets at $\delta 12.0$ (t, $J_{P-F} = 8.3$, $J_{P-Rh} = 133.3$ Hz); the ^{19}F NMR spectrum shows two sets of equivalent fluorines at $\delta -98.2$ and -113.7 .

Irradiation of 1 with 4-Dimethylamino-2,3,5,6-tetrafluoropyridine (c). The irradiation of **1** in hexane ($\lambda > 290$

nm, 8 h, room temperature) with the excess substituted tetrafluoropyridine 4-dimethylamino-2,3,5,6-tetrafluoropyridine (c) generates the metallacycle $\text{CpRh}(\text{PMe}_3)(\kappa^2\text{-C,C-CH}_2\text{N}(\text{CH}_3)_2\text{C}_5\text{NF}_3)$ (4) with an NMR yield of 85% (Scheme 4).

Scheme 4. Photochemical Reaction of 1 with c and d



When the reaction was scaled up, the complex crystallized out of the reaction mixture during photolysis as an isolable, air-stable, pale orange solid. The ^1H NMR spectrum shows the CH_2 protons of the metallacycle 4 to be diastereotopic, because it is bonded to a stereogenic Rh center. The two resonances are correlated by COSY NMR spectroscopy and appear at δ 3.04 (ddd) and at δ 4.87 (m) with different P–H and H–H coupling constants.

This very low field chemical shift for the diastereotopic proton compares with shifts of δ 6.82 and 5.24 for the diastereotopic proton of the complex $\text{CpRh}(\text{PMe}_3)(\kappa^2\text{-C,C-CH}_2\text{OC}_6\text{F}_4)$ previously observed.¹⁷ The $^{31}\text{P}\{^1\text{H}\}$ NMR spectrum displays a doublet with a coupling constant typical of a Rh(III) species (δ 13.8, $J_{\text{PRh}} = 158$ Hz).^{15b} The ^{19}F NMR spectrum displays three different peaks for the three inequivalent fluorines, two at lower field for the fluorines ortho to nitrogen and one at higher field. Finally, the ^{13}C DEPT spectrum of 4 confirms that the resonance at δ 40.3 arises from a CH_2 group (dd $J_{\text{CRh}} = 29.8$ Hz, $J_{\text{CP}} = 13.8$ Hz). A complete set of chemical shifts and coupling constants is given in Table 1.

Complex 4 was isolated as small pale orange crystals by crystallization from hexane, and its structure was determined by X-ray crystallography (Figure 3). The five-membered rhodacycle is planar, as confirmed by the sum of the internal angles (539.89°). It is also coplanar with the pyridine ring fused to it.

Irradiation of 1 with 4-Methoxy-2,3,5,6-tetrafluoropyridine (d). The irradiation of 1 in hexane ($\lambda > 290$ nm, 6 h, room temperature) with excess substituted tetrafluoropyridine 4-methoxy-2,3,5,6-tetrafluoropyridine (d) generates the metallacycle $\text{CpRh}(\text{PMe}_3)(\kappa^2\text{-C,C-CH}_2\text{OC}_5\text{NF}_3)$ (5) with an NMR yield of 20%. The formation of 5 appeared to be limited by a dark film formed on the wall of the tube. Low-temperature (-20°C) photolysis and use of a $\lambda > 350$ nm UV filter did not improve the conversion. The ^1H NMR spectrum again shows the CH_2 protons of the metallacycle 5 to be diastereotopic. The two resonances appeared at lower field than those observed for 4: δ 5.25 (ddd) and 6.90 (m). Complex 5 was isolated as small pale orange crystals by crystallization from hexane. A crystal structure determination was attempted, but the refinement never converged satisfactorily because of twinning. Nevertheless, the identity of complex 5 was confirmed.

Thermal Reactions of $\text{CpRh}(\text{PMe}_3)(\text{Ph})\text{H}$ (6) with a–d. The irradiation of 1 in neat C_6H_6 formed the C–H activated product $\text{CpRh}(\text{PMe}_3)(\text{Ph})\text{H}$ (6), as previously reported.¹⁶

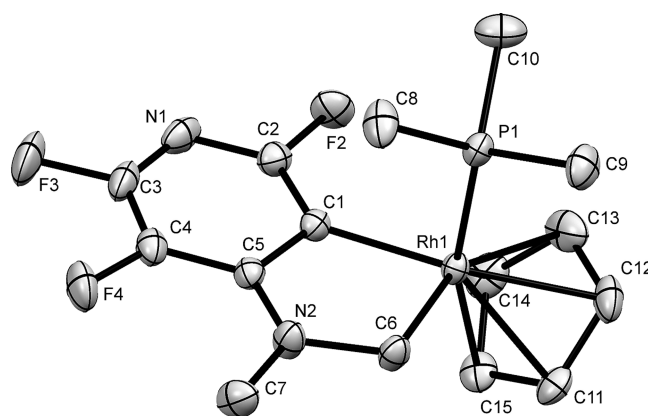


Figure 3. Molecular structure of 4. Principal bond distances (Å): C(1)–Rh(1) 2.023(3), C(6)–Rh(1) 2.069(3), Rh(1)–P(1) 2.2311(7), C(1)–C(5) 1.422(3), C(6)–N(2) 1.463(3), C(5)–N(2) 1.346(3). Principal angles (deg): P(1)–Rh(1)–C(6) 89.60(8), P(1)–Rh(1)–C(1) 87.87(7). Hydrogen atoms are omitted for clarity. Ellipsoids for the anisotropic displacement parameters are shown at the 50% level.

Complex 6 was used as a precursor to check if its thermal reactivity in hexane with excess fluoropyridines (10-fold) resulted in the same product distribution. The reaction of 6 with a at 50°C was completed overnight to form complex 2 as the principal product. Conversion of 6 to complex 3 by reaction with b also proceeded under the same reaction conditions; an additional unidentified phosphorus-containing species was observed by $^{31}\text{P}\{^1\text{H}\}$ NMR spectroscopy. The same route was explored for complex 6 with excess c and d. The formation of the metallacycles 4 and 5 was confirmed along with the appearance of a mixture of unidentified side products observable by ^{19}F and ^1H nuclei spectroscopy. The new set of products, which were not observed by the photochemical route, remained unidentified.

Mechanistic Studies. a. Reaction with Pentafluoropyridine. Photochemical reaction of complex 1 with pentafluoropyridine produces a mixture of compounds: complex 2 was identified as the only one with a coupling constant J_{PRh} characteristic of Rh(I); all the rest are Rh(III) species. The selectivity toward formation of 2 was achieved by performing photolysis at low temperature in hexane with a 10-fold excess of pentafluoropyridine. Variable-temperature NMR spectroscopy (210–320 K) was performed in order to look for any other isomers, but no new compounds were detected, confirming that the reaction is regioselective toward the C(3)–C(4) position. When the reaction was monitored in situ, a hydride resonance was detected at δ -12.42 (dd, $J_{\text{P-H}} = 39.9$ Hz, $J_{\text{Rh-H}} = 22.9$ Hz) which was identical to the hydride resonance of 3. Probably, reaction of C_5NF_5 with some species formed in the reaction mixture led to hydrodefluorination to form $\text{C}_5\text{NF}_4\text{H}$ as already reported.²⁵ It is clear from these experiments that complex 2 is stabilized enough for isolation and that C–F oxidative addition certainly does not occur under mild conditions. The complex appeared to be stable in solution upon heating up to 100°C . The reaction of 1 with 2,3,5,6-tetrafluoropyridine produces the C–H activation product cleanly in 100% NMR yield. Even when the irradiation was prolonged, no evidence for C–F activation was found and complex 3 was the only observed product.

b. Reaction of Complex 1 with 4-Substituted Tetrafluoropyridines. The photoreaction of 1 with 4-substituted

tetrafluoropyridines C_5NF_4X ($X = OMe, NMe_2$) yields metallacycles **4** and **5**. We also investigated these reactions in NMR experiments to search for reaction intermediates. The expected byproduct, free HF, was observed in the 1H NMR spectrum as a low-field broad peak at δ 14.7 (see the Supporting Information). The photochemical reaction of **1** results in initial photodissociation of C_2H_4 from **1**;¹⁶ possible reaction intermediates could arise by coordination of the substrate by η^2 coordination and/or C–F or C–H oxidative addition. The formation of **4** and **5** by thermal reaction of $CpRh(PMe_3)(Ph)H$ with **c** and **d** confirms that the photochemical step is elimination of C_2H_4 from **1** (see the Introduction) and that the remaining steps are thermal in origin. When the reaction is conducted in hexane or in cyclohexane- d_{12} and followed by 1H NMR spectroscopy, a hydride is detected at δ –14 (dd, $J_{P-H} = 38.6$, $J_{Rh-H} = 28.9$ Hz) as a minor product in addition to the metallacycle. The hydride was identified as $CpRh(PMe_3)_2H$ by comparison with previous work.²⁶ When the reaction was followed by ^{31}P and ^{19}F NMR spectroscopy, we did not notice any evidence of a Rh(I) complex characteristic of η^2 coordination or a ^{19}F resonance at high field characteristic of a fluoride complex. Even when the reaction was carried out at 253 K and the NMR spectrum taken at 200 K, no such species were observed. In contrast, it was established previously that cyclometalation occurred via η^2 coordination on photoreaction of **1** with C_6F_5OMe .^{16,17}

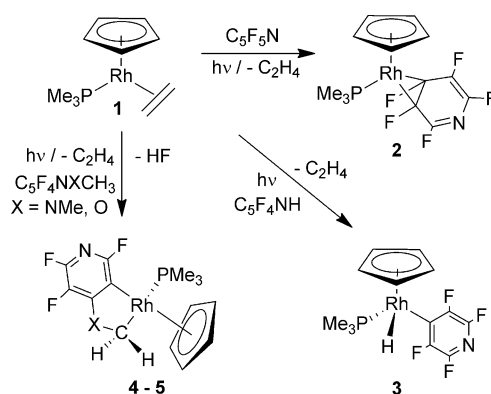
In order to elucidate the role of the substituent on the fluoropyridine ring, we also examined the photoreactions of **1** with 4-ethyltetrafluoropyridine and with 4-ethoxytetrafluoropyridine. Neither reaction showed any cyclometalated products. We conclude that cyclometalation requires a heteroatom substituent and a primary C–H bond as in $-NMe_2$ or $-OMe$. The preference for the metal center to activate a primary C–H bond has already been observed by Jones et al.²⁷ We also investigated the addition of CsF as a base to trap HF: it neither promoted the formation of the cyclometalated species nor inhibited it. However, we note that a weak base is present in the form of excess 4-substituted pyridine (see the Discussion).

The kinetic isotopic effect was also explored. A large isotopic effect was reported for an Ir-PCP/4-methoxy-2,3,5,6-tetrafluorotoluene system to form the C–O activated product where neither a direct oxidative addition nor a simple SN_2 mechanism was observed.²⁸ The deuterated analogue of 2,3,5,6-tetrafluoro-4-methoxypyridine, $C_5NF_4OCD_3$, was synthesized and characterized by NMR spectroscopy, mass spectrometry, and IR absorption (see the Supporting Information). The irradiation of **1** in hexane with excess of both substituted tetrafluoropyridines **d** and **d**- OCD_3 , present in a 1:5:5 ratio ($\lambda > 290$ nm, 12 h, room temperature) generates a mixture of the metallacycles $CpRh(PMe_3)(\kappa^2-C,C-CH_2OC_5NF_3)$ (**5**) and the deuterated analogue $CpRh(PMe_3)(\kappa^2-C,C-CD_2OC_5NF_3)$ (**6**) with an NMR yield of 30%. Since the ^{19}F and $^{31}P\{^1H\}$ NMR spectra of the two cyclometalated species are coincident, EI mass spectrometry was employed to determine the KIE. Reproducible results were obtained from two parallel experiments that showed a product ratio of 0.94 ± 0.04 . We conclude that the KIE is very small.

DISCUSSION

The reactions of **1** with fluorinated pyridines are summarized in Scheme 5. The current experiments demonstrate the formation by photochemical reaction of $CpRh(PMe_3)(\eta^2-C_3C_4-C_5NF_5)$

Scheme 5. Reactions of Complex **1** with Fluorinated Pyridines



as an isolable solid. Reaction with 2,3,5,6-tetrafluoropyridine is selective for C–H activation. Use of NMe_2 and OMe substituents on the fluoropyridine results in cyclometalation to form new air-stable rhodacycle species by both C–H and C–F insertion (Scheme 5).

Pentafluoropyridine is a weak nitrogen base. According to DFT calculations, the HOMO is the a_2 ring π orbital with a node through nitrogen, and the nitrogen lone pair appears as the HOMO-1 or HOMO-2 (according to the method). The LUMO is the $3b_1$ π^* orbital.²⁹ The photoreaction of **1** with pentafluoropyridine to form the η^2 -C,C-coordinated complex **2** may be contrasted with other reactions of pentafluoropyridine, which reveal a wide variety of modes of coordination and activation. The reaction of $(dfepe)PtMe_2$ with $(1,3,5-C_6H_4Me_3)^+B(C_6F_5)_4^-$ ($dfepe = (C_2F_5)_2PCH_2CH_2P(C_2F_5)_2$) in the presence of C_5NF_5 and that of $[(tmeda)Pt(CH_3)_2]$ ($tmeda = N,N,N',N'$ -tetramethylethylenediamine) with $[C_5NF_5H]BARF_4$ yield N-coordinated products.^{22a,b} Nitrogen coordination of pentafluoropyridine was also observed for $cis-[Re(PR_3)(CO)_4(L)][BARF_4]$ ³⁰ and $[CF_3PCPPT(C_5NF_5)]^+$ (where $CF_3PCP = (1,3-C_6H_4(CH_2P(CF_3)_2)_2)$).³¹ C–F oxidative addition takes place on reaction of $Ni(COD)_2$ in the presence of excess of PEt_3 and pentafluoropyridine, leading preferentially to an ortho-activated $trans-Ni(F)(2-C_5NF_4)(PEt_3)_2$ complex.³² However, the activation takes place at the para position when the phosphine is replaced by a carbene.³⁵ DFT calculations based on the model $Ni(PMe_3)_2$ suggest that the ortho regioselectivity derives from a neighboring group effect with participation of the phosphine and the nitrogen of the pentafluoropyridine.³⁴ Johnson explored the reactivity of the phenanthrene adduct $(PEt_3)_2Ni(\eta^2-C_{14}H_{10})$ toward pentafluoropyridine; both the mononuclear adduct $(PEt_3)_2Ni(\eta^2-C,C-C_5NF_5)$ and the analogous dinuclear adduct $[(PEt_3)_2Ni]_2(\mu-\eta^2-\eta^2-C,C-C_5NF_5)$ were characterized in solution, confirming that coordination precedes C–F activation.²³ Para C–F activation of pentafluoropyridine with $Pt(PCy_3)_2$ and $Pd(PCy_3)_2$ forms the tetrafluoropyridyl products through two different mechanisms: phosphine assistance for the platinum complex and C–F oxidative addition for the palladium species.³⁵

In order to explore the preference for C–H compared to C–F activation, the reaction of complex **1** with 2,3,5,6-tetrafluoropyridine was investigated. It produces the C–H activated product **3** cleanly, in contrast to $Ni(COD)_2$, where C–F activation was preferred to form the ortho C–F activated species as the major product.³² Recently Johnson and co-

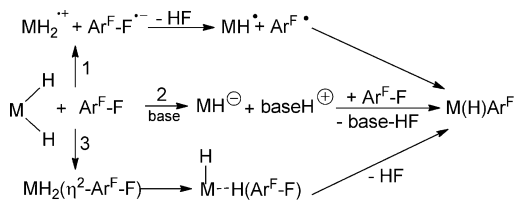
workers isolated the C–H activated product of tetrafluoropyridine as the major species for reaction of the phenanthrene adduct $(\text{PEt}_3)_2\text{Ni}(\eta^2\text{-C}_{14}\text{H}_{10})$ at temperatures lower than 193 K, demonstrating that small changes in reaction conditions could drastically influence the selectivity.²³

The introduction of an NMe_2 or OMe substituent on the pyridine leads to cyclometalation by C–F and C–H activation with concomitant elimination of HF. The role played by the substituent is crucial in reactions of complex **1** with 4-substituted fluorinated pyridines. Different reactivity is shown employing complex **1** in reactions with ethoxy- and ethyl-tetrafluoropyridines, showing that the complex needs a primary carbon as in OMe or NMe_2 to cyclometalate as well as the presence of the heteroatom on the substituent. In contrast, the same pyridines react at $\text{Ni}(\text{PEt}_3)_2$ to give C–F oxidative addition at the 2-position, reactivity analogous to that shown by pentafluoropyridine toward $\text{Ni}(\text{PEt}_3)_2$.³⁶

To our knowledge, there are few reported reactions which eliminate HF from a single substrate in a manner similar to the cyclometalation reactions above. Since HF has an exceptionally large bond dissociation energy, its formation will act as a thermodynamic driver. The reaction is likely to be initiated by coordination of the 4-substituted pyridine, followed by either C–F oxidative addition or C–H oxidative addition. It was already established that the $\text{CpRh}(\text{PMe}_3)$ fragment selectively activates C–H bonds over C–F bonds.²⁰ The C–F oxidative addition product with hexafluorobenzene was observed only in low-temperature matrices.¹⁹ η^2 coordination takes place for the reaction of the same Rh fragment with methoxypentafluorobenzene. The reaction then proceeds through a cyclometalation pathway, liberating HF (Scheme 1). Displacement of HF and ring closure gives rise to the cyclometalated species, but the detailed mechanism of HF elimination is unknown.¹⁷

Three mechanisms have been proposed to explain the formation of HF in related reactions: electron transfer or nucleophilic attack of two different types (Scheme 6). Notably,

Scheme 6. Mechanism Where HF Is Eliminated To Form the Products: (1) Electron Transfer; (2) Base-Assisted Nucleophilic Substitution; (3) Ortho-Selective Nucleophilic Attack



all three reactions start from metal hydride complexes. $\text{Ru}(\text{dmpe})_2\text{H}_2$ was proposed to react at -78°C with hexafluorobenzene to give the pentafluorophenyl hydride complex through an electron-transfer process where HF is lost (Scheme 6, path 1).³⁷ $\text{Cp}^*\text{Rh}(\text{PMe}_3)\text{H}_2$ activates the C–F bond of a variety of fluoroaromatics thermally by a nucleophilic aromatic substitution. Either pyridine or fluoride acts as base to produce the metal anion, the active species in the C–F activation. HF is produced in this reaction together with the C–F activated product (Scheme 6, path 2).³⁸ Recently, DFT studies on the reaction of $\text{Ru}(\text{NHC})(\text{PPh}_3)(\text{CO})\text{H}_2$ in the presence of fluorinated arenes indicated a novel mechanism where a metal hydride reacts intermolecularly with $\text{C}_6\text{F}_5\text{H}$ by

ortho-selective nucleophilic attack to form HF (Scheme 6, path 3).³⁹

All of these examples suggest that the cyclometalation reactions described here proceed via C–H bond activation of 4-substituted pyridines at the NMe_2 or OMe groups, even though we have not detected a significant KIE. Distinction between the three mechanisms outlined in Scheme 6 is not possible. A similar problem of the order of C–H and C–F bond activation is apparent in the photochemical reaction of $\text{Cp}^*\text{Re}(\text{CO})_3$ with hexafluorobenzene. This reaction results in insertion into the C–F bond with concomitant C–H activation of a methyl of the Cp^* ligand to form $\text{Re}(\eta^6\text{-C}_5\text{Me}_4\text{CH}_2)(\text{CO})_2(\text{C}_6\text{F}_5)$ with HF elimination, but the mechanism is unknown.⁴⁰ Hydrodefluorination is usually carried out with fluoride acceptors such that generation of HF is avoided.¹¹

CONCLUSIONS

The behavior of transition-metal complexes toward fluorinated pyridines is remarkably diverse. In this paper, we have studied the reactivity of photochemically generated $\text{CpRh}(\text{PMe}_3)$ toward fluorinated pyridines. Pentafluoropyridine coordinates to $\text{CpRh}(\text{PMe}_3)$ in an $\eta^2\text{-C,C}$ mode, providing a crystallographically characterized example of a coordination mode implicated previously by NMR spectroscopy and by DFT calculations. In contrast, 2,3,5,6-tetrafluoropyridine undergoes C–H oxidative addition. The corresponding tetrafluoropyridine containing an NMe_2 or OMe group at the 4-position reacts to form a cyclometalated product via combined C–H and C–F bond activation with HF elimination. These reactions contrast with the behavior of the same reagents toward rhenium, nickel, and platinum complexes, as discussed in detail above.

EXPERIMENTAL SECTION

General Procedures. All operations were performed under an argon atmosphere, on a high-vacuum line (10^{-4} mbar) using modified Schlenk techniques, on standard Schlenk (10^{-2} mbar) lines, or in a glovebox. Solvents for general use (hexane, benzene) were of AR grade, dried by distillation over classical reagents, and stored under Ar in ampules fitted with Young PTFE stopcocks. Hexane was collected from the purification system and dried again by distillation. Deuterated solvents were dried by stirring over potassium and were distilled under high vacuum into small ampules with potassium mirrors. Pentafluoropyridine and 2,3,5,6-tetrafluoropyridine were purchased from Sigma-Aldrich and dried over molecular sieves. Photochemical reactions, at room temperature, were performed in glass NMR tubes fitted with PTFE taps, using a 125 W medium-pressure mercury vapor lamp with a water filter (5 cm). UV–vis irradiation at lower temperatures was performed using a 300 W Oriel 66011 xenon lamp with a thermostatically controlled cooling system cooled by gaseous nitrogen boil-off. All NMR spectra were recorded on Bruker AMX500 spectrometers in glass tubes fitted with Young PTFE stopcocks. All ^1H and ^{13}C chemical shifts are reported relative to tetramethylsilane and are referenced using the chemical shifts of residual protio solvent resonances (benzene, δ 7.15 for ^1H and δ 128.0 for ^{13}C). ^{19}F NMR spectra were recorded at 470.5 MHz and referenced to external CFCl_3 at δ 0. The $^{31}\text{P}\{^1\text{H}\}$ NMR spectra were recorded at 202.5 MHz and are referenced to external H_3PO_4 . EI mass spectra were measured on a Waters Micromass GCT Premier orthogonal time-of-flight instrument. The LIFDI mass spectra were measured on the same instrument set to one scan per second with resolution power of 6000 fwhm and equipped with a LIFDI probe from LINDEN GmbH. The design is very similar to that described by Gross et al.⁴¹ Toluene was used for tuning the instrument. The poly(ethylene glycol) probe was kept at ambient temperature with the emitter potential at 12 kV. Activated tungsten wire LIFDI emitters (13 μm tungsten from LINDEN) were ramped manually up to 100 mA for

the emitter heating current during the experiment. m/z values are accurate to 0.01 Da. The IR experiments were performed using a Unicam RS 10000E FTIR instrument. The spectrum was recorded on a liquid film averaging 16 scans at 1 cm^{-1} resolution.

Diffraction data for $\text{CpRh}(\text{PMe}_3)(\eta^2\text{-C}_5\text{NF}_5)$ were collected at 110 K on a Bruker Smart Apex diffractometer with Mo $K\alpha$ radiation ($\lambda = 0.71073\text{ \AA}$) using a SMART CCD camera. Diffractometer control, data collection, and initial unit cell determination was performed using SMART (v5.625 Bruker-AXS). Frame integration and unit-cell refinement software was carried out with SAINT+ (v6.22, Bruker AXS). Absorption corrections were applied using SADABS (v2.03, Sheldrick). The structure was solved by direct methods using SHELXS-97 (Sheldrick, 1997) and refined by full-matrix least squares using SHELXL-97 (Sheldrick, 1997).⁴² Diffraction data for $\text{CpRh}(\text{PMe}_3)(\kappa^2\text{-C,C-CH}_2\text{N}(\text{CH}_3)\text{C}_5\text{NF}_5)$ and $\text{CpRh}(\text{PMe}_3)(\text{C}_5\text{NF}_4)\text{H}$ were collected at 110 K on an Agilent SuperNova diffractometer with Mo $K\alpha$ radiation ($\lambda = 0.71073\text{ \AA}$). Data collection, unit cell determination, and frame integration were carried out with "CrystalisPro". Absorption corrections were applied using crystal face indexing and the ABSPACK absorption correction software within CrystalisPro. Structures were solved and refined using Olex2⁴³ implementing SHELX algorithms. Structures were solved by either Patterson or direct methods using SHELXS-97 and refined by full-matrix least squares using SHELXL-97. All non-hydrogen atoms were refined anisotropically. Carbon-bound hydrogen atoms were placed at calculated positions and refined using a "riding model". Crystallographic parameters for 2–4 are given in Table S1 (Supporting Information).

Synthesis and NMR Experiments. $\text{CpRh}(\text{PMe}_3)(\text{C}_2\text{H}_4)$ was synthesized by literature procedures, but replacing TICp by LiCp.⁴⁴ 4-Dimethylamino-2,3,5,6 tetrafluoropyridine and 4-methoxy-2,3,5,6-tetrafluoropyridine were also synthesized by literature procedures.⁴⁵ The pyridines were additionally characterized by NMR spectroscopy and EI mass spectrometry. NMR yields were determined by ³¹P NMR spectroscopy as product integration/total integration.

Preparation of $\text{CpRh}(\text{PMe}_3)(\eta^2\text{-C}_5\text{NF}_5)$ (2). An 8 mm diameter NMR tube, fitted with a Young tap, was charged with complex 1 (50 mg) and pentafluoropyridine (2 fold excess) in hexane and irradiated at $-20\text{ }^\circ\text{C}$ with the Oriel Xe arc (8 h), resulting in 60% conversion to 2. The excess of pentafluoropyridine and solvent were pumped down under vacuum, and part of the unreacted starting material and other products were sublimed at $25\text{ }^\circ\text{C}$ and 1×10^{-4} mbar onto a liquid nitrogen cold finger, leaving a brown residue. The brown residue was suspended in dry hexane, heated to $60\text{ }^\circ\text{C}$, and filtered under argon. The orange solution was then cooled to $-20\text{ }^\circ\text{C}$ for a few days to obtain small orange crystals of complex 2.

¹H NMR (C_6D_6 , 300 K): δ 4.37 (s, 5H, C_5H_5), 0.79 (d, 9H, $J_{\text{P-H}} = 10.6\text{ Hz}$, PMe_3). ³¹P{¹H} NMR: δ 3.09 (ddd, $J_{\text{Rh-P}} = 192$, $J_{\text{P-F}} = 56$, $J_{\text{P-C}} = 52\text{ Hz}$). ¹³C{¹H} NMR: δ 91.44 (t, C_5H_5), 21.90 (d, $J_{\text{P-C}} = 31\text{ Hz}$, PMe_3); there is no indication in the spectrum of carbons corresponding to the pentafluoropyridine ring. ¹⁹F NMR: δ -55.5 (m, 1F, F_2), -119.8 (t, $J_{\text{F-F}} = 11.4$, 1F, F_6), -155.7 (tdd, $J_{\text{F-F}} = 11.4$, 15.3, 34.3 Hz, 1F, F_5), -157.3 (m, 1F, F_4), -169.0 (m, 1F, F_3). EI MS: m/z 412.9876 (M^+) 100% (calcd for $\text{C}_{13}\text{H}_{14}\text{NF}_5\text{PRh}$ 412.9839, difference 0.4 mDa).

Preparation of $\text{CpRh}(\text{PMe}_3)(\text{C}_5\text{NF}_4)\text{H}$ (3). An NMR tube, fitted with a Young tap, was charged with complex 1 (15 mg) and 2,3,5,6-tetrafluoropyridine (2-fold excess) in C_6D_{12} and irradiated at room temperature (8 h), resulting in 100% conversion to 3.

¹H NMR (C_6D_{12} , 300 K): δ 5.25 (s, 5H, C_5H_5), 1.35 (d, $J_{\text{P-H}} = 13\text{ Hz}$, 9H, PMe_3), -12.42 (dd, $J_{\text{P-H}} = 40$, $J_{\text{Rh-H}} = 23\text{ Hz}$, 1H, Rh-H). ³¹P{¹H} NMR: δ 11.1 (dd, $J_{\text{Rh-P}} = 142$, $J_{\text{F-P}} = 22\text{ Hz}$). ¹³C{¹H} NMR: δ 87.46 (t, $J_{\text{C-P}} = 3\text{ Hz}$, C_5H_5), 21.71 (dd, $J_{\text{C-P}} = 35$, $J_{\text{C-Rh}} = 1.4\text{ Hz}$, PMe_3); there is no indication in the spectrum of carbons corresponding to the tetrafluoropyridine ring. ¹⁹F NMR: δ -100.67 (m, 2F, F meta to Rh), -113.7 (m, 2F, F ortho to Rh). MS (LIFDI, m/z): 395.01 (100%, M^+), 393.99 (20%, [M^+] - HF) exptl; 394.99 calcd for $\text{C}_{13}\text{H}_{15}\text{NPF}_4\text{Rh}$. Anal. Calcd for $\text{C}_{13}\text{H}_{15}\text{NPF}_4\text{Rh}$: 0.15 $\text{C}_5\text{F}_4\text{NH}$: C, 39.53; H, 3.65; N, 3.86. Found: C, 39.76; H, 3.73; N, 4.16.

Preparation of $\text{CpRh}(\text{PMe}_3)(\text{C}_5\text{NF}_4)\text{Cl}$ (3-Cl). A solution of 1 and 2,3,5,6-tetrafluoropyridine in 0.5 mL of hexane was irradiated in an NMR tube as described previously. Volatiles were then removed under vacuum, and the residue was redissolved in hexane. This solution was added to carbon tetrachloride (1 mL) under inert conditions at $-20\text{ }^\circ\text{C}$. The mixture was maintained at $-20\text{ }^\circ\text{C}$ for 3 h, after which point the solvent was removed under vacuum. The crude product was dissolved in C_6D_6 to obtain NMR characterization data.

¹H NMR (C_6D_6 , 300 K): δ 4.50 (d, $J_{\text{Rh-H}} = 1.6\text{ Hz}$, 5H, C_5H_5), δ 1.04 (d, $J_{\text{P-H}} = 11.8\text{ Hz}$, 9H, PMe_3). ³¹P{¹H} NMR: δ 12.0 (dt, $J_{\text{Rh-P}} = 133$, $J_{\text{F-P}} = 9\text{ Hz}$). ¹³C{¹H} NMR: δ 88.7 (dd, $J = 3$, 4 Hz, C_5H_5), δ 17.9 (dd, $J_{\text{C-P}} = 35\text{ Hz}$, PMe_3). ¹⁹F NMR: δ -98.20 (m, 2F, F_3 , F_4), δ -113.7 (m, 2F, F_2 , F_5). MS (LIFDI, m/z): 428.95 (100%, M^+) exptl; 428.95 calcd for $\text{C}_{13}\text{H}_{14}\text{NClPF}_4\text{Rh}$. EI MS: m/z 428.9544 (M^+) 40% (calcd for $\text{C}_{13}\text{H}_{14}\text{N}^{35}\text{ClPF}_4\text{Rh}$ 428.9544, difference 0.0 mDa), 392.9733 (100%, [M^+] - Cl).

Preparation of $\text{CpRh}(\text{PMe}_3)(\kappa^2\text{-C,C-CH}_2\text{N}(\text{CH}_3)\text{C}_5\text{NF}_3)$ (4). An 8 mm diameter NMR tube, fitted with a Young tap, was charged with complex 1 (50 mg) and previously degassed 4-dimethylamino-2,3,5,6-tetrafluoropyridine (5-fold excess) in hexane and irradiated at room temperature (8 h), resulting in 85% conversion to 4. The excess of pyridine and solvent were pumped down under vacuum, and part of the unreacted starting material and other byproducts were sublimed at $25\text{ }^\circ\text{C}$ and 1×10^{-4} mbar onto a liquid nitrogen cold finger, leaving a sticky brown residue. The brown residue was then washed with hexane (three times), dried, and dissolved in C_6D_6 in order to obtain NMR characterization data. Pure crystals appeared as light orange blocks at low T ($-20\text{ }^\circ\text{C}$) from dry hexane. Suitable material for elemental analysis was obtained by washing the solid with a cold mixture of degassed ethanol and water.

¹H NMR (C_6D_6 , 300 K): δ 4.98 (dd, CH_2 , H_b , $J_{\text{H-Rh}} = 5$, $J_{\text{H-H}} = 7\text{ Hz}$), 4.87 (d, $J_{\text{Rh-H}} = 1\text{ Hz}$, C_5H_5), 3.04 (ddd, CH_2 , H_a , $J_{\text{P-H}} = 2$, $J_{\text{Rh-H}} = 7$, $J_{\text{H-H}} = 16\text{ Hz}$), 2.96 (d, CH_3 , $J_{\text{H-H}} = 3\text{ Hz}$), 0.65 (d, $J_{\text{P-H}} = 11\text{ Hz}$, PMe_3). ³¹P{¹H} NMR: δ 13.8 (d, $J_{\text{Rh-P}} = 158\text{ Hz}$). ¹³C{¹H} NMR: δ 89.5 (t, $J_{\text{C-P}} = 3\text{ Hz}$, C_5H_5), 40.3 (ddd, $J_{\text{C-Rh}} = 30$, $J_{\text{C-P}} = 15$, $J_{\text{C-C}} = 1\text{ Hz}$, CH_2), 38.9 (dd, $J_{\text{C-P}} = 12$, $J_{\text{C-C}} = 2\text{ Hz}$, CH_3), 17.5 (d, $J_{\text{C-P}} = 32\text{ Hz}$, PMe_3). ¹⁹F NMR: δ -66.5 (dd, $J_{\text{F-F}} = 13$, 24 Hz, F_2), -100.1 (dd, $J_{\text{F-F}} = 13$, 24 Hz, F_3), -180.2 (t, $J_{\text{F-F}} = 24\text{ Hz}$, F_4). EI MS: m/z 418.0299 (M^+) 100% (calcd for $\text{C}_{15}\text{H}_{19}\text{N}_2\text{F}_3\text{PRh}$ 418.0293, difference 0.6 mDa). IR (solid): ν (CF stretching and ring vibration)/ cm^{-1} 1600 (m), 1578 (m), 1435 (m), 0.1411 (m), 1339 (m), 1299 (m), 1288 (m), 1257 (w), 1180 (w), 1167 (m), 1145 (m), 1039 (m), 1018 (m), 1018 (m), 950 (s), 938 (s), 888 (w), 820 (m), 804 (s), 734 (m), 718 (m), 680 (m). Anal. Calcd for $\text{C}_{15}\text{H}_{19}\text{N}_2\text{F}_3\text{PRh}$: C, 43.08; H, 4.58; N, 6.70. Found: C, 43.21; H, 4.56; N, 6.54.

Preparation of $\text{CpRh}(\text{PMe}_3)(\kappa^2\text{-C,C-CH}_2\text{OC}_5\text{NF}_3)$ (5). An 8 mm diameter NMR tube, fitted with a Young tap, was charged with complex 1 (50 mg) and previously degassed 4-methoxy-2,3,5,6-tetrafluoropyridine (5-fold excess) in hexane and irradiated at room temperature (6 h), resulting in 20% conversion to 4. The excess of pyridine and solvent were pumped down under vacuum, and part of the unreacted starting material and other byproducts were sublimed at $25\text{ }^\circ\text{C}$ and 1×10^{-4} mbar onto a liquid nitrogen cold finger, leaving a brown sticky residue. The brown residue was then washed with hexane (three times), dried, and dissolved in C_6D_6 in order to obtain NMR characterization data. Crystals appeared as light orange blocks at low T ($-20\text{ }^\circ\text{C}$) from dry hexane.

¹H NMR (C_6D_6 , 300 K): δ 6.77 (dt, CH_2 , 1H, H_b , $J_{\text{H-H}} = 5$, $J_{\text{H-Rh}} = 1\text{ Hz}$), 5.1 (ddd, CH_2 , 1H, H_a , $J_{\text{P-H}} = 1$, $J_{\text{Rh-H}} = 6$, $J_{\text{H-H}} = 18\text{ Hz}$), 4.73 (d, $J_{\text{Rh-H}} = 1\text{ Hz}$, 5H, C_5H_5), 0.55 (d, $J_{\text{P-H}} = 10\text{ Hz}$, 9H, PMe_3). ³¹P{¹H} NMR: δ 14.0 (d, $J_{\text{Rh-P}} = 159\text{ Hz}$). ¹³C{¹H} NMR: δ 89.7 (t, $J_{\text{C-C}} = 3\text{ Hz}$, C_5H_5), 17.9 (d, $J_{\text{C-P}} = 33\text{ Hz}$, PMe_3), 41 (ddd, $J_{\text{C-Rh}} = 30$, $J_{\text{C-P}} = 14$, $J_{\text{C-C}} = 1\text{ Hz}$, CH_2). ¹⁹F NMR: δ -64.6 (dd, $J_{\text{F-F}} = 14$, 22 Hz, 1F, F_2), -99.1 (dd, $J_{\text{F-F}} = 14$, 22 Hz, 1F, F_3), -172.0 (t, $J_{\text{F-F}} = 22\text{ Hz}$, 1F, F_4). EI MS: m/z 404.9975 (M^+) 100% (calcd 404.9977, difference 0.2 mDa).

■ ASSOCIATED CONTENT

S Supporting Information

NMR spectra of complexes 2–5, IR spectra of 4, and preparation and characterization of $C_3F_4N(OCD_3)$. Information for all the crystal structures in CIF format are available free of charge via the Internet at <http://pubs.acs.org>.

■ AUTHOR INFORMATION

Corresponding Author

*E-mail: robin.perutz@york.ac.uk

Present Addresses

[†]School of Chemistry, University of East Anglia, Norwich Research Park, Norwich NR4 7TJ, U.K.

[‡]Instituto de Investigaciones Químicas, Avda. Américo Vespucio 49, 41092 Sevilla, Spain.

Notes

The authors declare no competing financial interest.

■ ACKNOWLEDGMENTS

We thank the EPSRC for support and Dr. Naser Jasim for experimental assistance.

■ REFERENCES

- (1) (a) Sun, A. D.; Love, J. A. *Dalton Trans.* **2010**, 39, 10362. (b) Amii, H.; Uneyama, K. *Chem. Rev.* **2009**, 109, 2119. (c) Torrens, H. *Coord. Chem. Rev.* **2005**, 249, 1957. (d) Braun, T.; Wehmeier, F. *Eur. J. Inorg. Chem.* **2011**, 613. (e) Kiplinger, J. L.; Richmond, T. G.; Osterberg, C. E. *Chem. Rev.* **1994**, 94, 373. (f) Clot, E.; Eisenstein, O.; Jasim, N.; Macgregor, S. A.; McGrady, J. E.; Perutz, R. N. *Acc. Chem. Res.* **2011**, 44, 333. (g) Meier, G.; Braun, T. *Angew. Chem., Int. Ed.* **2009**, 48, 1546. (h) Braun, T.; Perutz, R. N. *Chem. Commun.* **2002**, 2749. (i) Kuehnle, M. F.; Lentz, D.; Braun, T. *Angew. Chem., Int. Ed.* **2013**, 52, 3328. (j) Braun, T.; Perutz, R. N. In *Comprehensive Organometallic Chemistry III*; Crabtree, R. H., Mingos, D. M. P., Eds.; Elsevier: Amsterdam, 2006; Vol. 1, Chapter 26. (k) Keyes, I.; Love, J. A. In *C–H and C–X Bond Functionalization: Transition Metal Mediation*; Ribas, X., Ed.; Royal Society of Chemistry: London, 2013; RSC Catalysis Series 11, pp 159–192.
- (2) Albrecht, M. *Chem. Rev.* **2010**, 110, 576.
- (3) (a) Pratihari, J. L.; Pattanayak, P.; Patra, D.; Rathore, R.; Chattopadhyay, S. *Inorg. Chim. Acta* **2011**, 367, 182. (b) Sunkel, K.; Graf, M.; Bottcher, H. C.; Salert, B.; Kruger, H. *Inorg. Chem. Commun.* **2011**, 14, 539. (c) Bottcher, H. C.; Graf, M.; Sunkel, K.; Salert, B.; Kruger, H. *Inorg. Chem. Commun.* **2011**, 14, 377.
- (4) Guard, L. M.; Ledger, A. E. W.; Reade, S. P.; Ellul, C. E.; Mahon, M. F.; Whittlesey, M. K. *J. Organomet. Chem.* **2011**, 696, 780.
- (5) Wu, W. T.; Wu, W. H.; Ji, S. M.; Guo, H. M.; Zhao, J. Z. *Dalton Trans.* **2011**, 40, 5953.
- (6) Pandiarajan, D.; Ramesh, R. *Inorg. Chem. Commun.* **2011**, 14, 686.
- (7) Li, X. Y.; Sun, H. J.; Yu, F. L.; Florke, U.; Klein, H. F. *Organometallics* **2006**, 25, 4695.
- (8) Lian, Z.; Xu, X. F.; Sun, H. J.; Chen, Y.; Zheng, T. T.; Li, X. Y. *Dalton Trans.* **2010**, 39, 9523.
- (9) Arroyo, M.; Bernes, S.; Ceron, M.; Cortina, V.; Mendoza, C.; Torrens, H. *Inorg. Chem.* **2007**, 46, 4857.
- (10) Wang, T. G.; Love, J. A. *Organometallics* **2008**, 27, 3290.
- (11) Arisawa, M.; Suzuki, T.; Ishikawa, T.; Yamaguchi, M. *J. Am. Chem. Soc.* **2008**, 130, 12214.
- (12) Noveski, D.; Braun, T.; Neumann, B.; Stammer, A.; Stammer, H. G. *Dalton Trans.* **2004**, 4106.
- (13) Teltewskoi, M.; Panetier, J. A.; Macgregor, S. A.; Braun, T. *Angew. Chem., Int. Ed.* **2010**, 49, 3947.
- (14) Pachal, S. R.; Saunders, G. C.; Weston, J. K. *Inorg. Chim. Acta* **2013**, 394, 558.
- (15) (a) Partridge, M. G.; McCamley, A.; Perutz, R. N. *J. Chem. Soc., Dalton Trans.* **1994**, 3519. (b) Campian, M. V.; Harris, J. L.; Jasim, N.;

Perutz, R. N.; Marder, T. B.; Whitwood, A. C. *Organometallics* **2006**, 25, 5093.

(16) Belt, S. T.; Duckett, S. B.; Helliwell, M.; Perutz, R. N. *J. Chem. Soc., Chem. Commun.* **1989**, 928.

(17) Ballhorn, M.; Partridge, M. G.; Perutz, R. N.; Whittlesey, M. K. *Chem. Commun.* **1996**, 961.

(18) Jones, W. D.; Partridge, M. G.; Perutz, R. N. *J. Chem. Soc., Chem. Commun.* **1991**, 264.

(19) Belt, S. T.; Helliwell, M.; Jones, W. D.; Partridge, M. G.; Perutz, R. N. *J. Am. Chem. Soc.* **1993**, 115, 1429.

(20) Selmeczy, A. D.; Jones, W. D.; Partridge, M. G.; Perutz, R. N. *Organometallics* **1994**, 13, 522.

(21) Higgitt, C. L.; Klahn, A. H.; Moore, M. H.; Oelckers, B.; Partridge, M. G.; Perutz, R. N. *J. Chem. Soc., Dalton Trans.* **1997**, 1269.

(22) (a) Basu, S.; Arulsamy, N.; Roddick, D. M. *Organometallics* **2008**, 27, 3659. (b) Holtcamp, M. W.; Henling, L. M.; Day, M. W.; Labinger, J. A.; Bercaw, J. E. *Inorg. Chim. Acta* **1998**, 270, 467.

(23) Hatnean, J. A.; Johnson, S. A. *Organometallics* **2012**, 31, 1361.

(24) Procacci, B. Ph.D. Thesis, University of York, 2012.

(25) Braun, T.; Noveski, D.; Ahijado, M.; Wehmeier, F. *Dalton Trans.* **2007**, 3820.

(26) Partridge, M. G. Ph.D. Thesis, University of York, 1992.

(27) (a) Tanabe, T.; Evans, M. E.; Brennessel, W. W.; Jones, W. D. *Organometallics* **2011**, 30, 834. (b) Vetter, A. J.; Jones, W. D. *Polyhedron* **2004**, 23, 413.

(28) (a) Choi, J.; Choliy, Y.; Zhang, X. W.; Emge, T. J.; Krogh-Jespersen, K.; Goldman, A. S. *J. Am. Chem. Soc.* **2009**, 131, 15627. (b) Kundu, S.; Choi, J.; Wang, D. Y.; Choliy, Y.; Emge, T. J.; Krogh-Jespersen, K.; Goldman, A. S. *J. Am. Chem. Soc.* **2013**, 135, 5127.

(29) Reinhold, M. Ph.D. Thesis, University of York, 2001; p 170.

(30) Huhmann-Vincent, J.; Scott, B. L.; Kubas, G. J. *Inorg. Chem.* **1999**, 38, 115.

(31) Adams, J. J.; Arulsamy, N.; Roddick, D. M. *Organometallics* **2009**, 28, 1148.

(32) Cronin, L.; Higgitt, C. L.; Karch, R.; Perutz, R. N. *Organometallics* **1997**, 16, 4920.

(33) (a) Schaub, T.; Fischer, P.; Steffen, A.; Braun, T.; Radius, U.; Mix, A. *J. Am. Chem. Soc.* **2008**, 130, 9304. (b) Doster, M. E.; Johnson, S. A. *Angew. Chem., Int. Ed.* **2009**, 48, 2185.

(34) Nova, A.; Reinhold, M.; Perutz, R. N.; Macgregor, S. A.; McGrady, J. E. *Organometallics* **2010**, 29, 1824.

(35) Jasim, N. A.; Perutz, R. N.; Whitwood, A. C.; Braun, T.; Izundu, J.; Neumann, B.; Rothfeld, S.; Stammer, H. G. *Organometallics* **2004**, 23, 6140.

(36) Dransfield, T. A.; Nazir, R.; Perutz, R. N.; Whitwood, A. C. *J. Fluorine Chem.* **2010**, 131, 1213.

(37) Whittlesey, M. K.; Perutz, R. N.; Moore, M. H. *Chem. Commun.* **1996**, 787.

(38) Edelbach, B. L.; Jones, W. D. *J. Am. Chem. Soc.* **1997**, 119, 7734.

(39) Panetier, J. A.; Macgregor, S. A.; Whittlesey, M. K. *Angew. Chem., Int. Ed.* **2011**, 50, 2783.

(40) Klahn, A. H.; Moore, M. H.; Perutz, R. N. *J. Chem. Soc., Chem. Commun.* **1992**, 1699.

(41) Gross, J. H.; Nieth, N.; Linden, H. B.; Blumbach, U.; Richter, F. J.; Tauchert, M. E.; Tompers, R.; Hofmann, P. *Anal. Bioanal. Chem.* **2006**, 386, 52.

(42) Sheldrick, G. M. *Acta Crystallogr., Sect. A: Found. Crystallogr.* **2008**, 64, 112.

(43) Dolomanov, O. V.; Bourhis, L. J.; Gildea, R. J.; Howard, J. A. K.; Puschmann, H. *J. Appl. Crystallogr.* **2009**, 42, 339.

(44) Werner, H.; Feser, R. *J. Organomet. Chem.* **1982**, 232, 351.

(45) Banks, R. E.; Burgess, J. E.; Cheng, W. M.; Haszeldine, R. N. *J. Chem. Soc.* **1965**, 575.